INTERNATIONAL JOURNAL of RENEWABLE ENERGY RESEARCH
M. Yahya et al., Vol.16, No.1, March, 2026

Improved Tilapia Fish Drying Products by Integrating Rotating Rack, Air Recirculation, and Heat Recovery Systems in the Greenhouse Solar Drying System

M. Yahya*‡, Putri Pratiwi*, Hafni*, Dedi Wardianto*, Asmara Yanto*

*Faculty of Industrial Technology, Institut Teknologi Padang, 25000 Padang, Indonesia

(yahya_err@yahoo.com, Pratiwi009@gmail.com, hafni@itp.ac.id, wardiantodedi71@gmail.com, asmarayanto@itp.ac.id)

‡Corresponding Author; M. Yahya, Faculty of Industrial Technology, Institut Teknologi Padang, 25000 Padang, Indonesia, Tel: +62 085274303960, yahya_err@yahoo.com.

Received: 12.12.2023 Accepted:08.02.2024

Abstract- A novel rotary rack-type greenhouse solar dryer (RRT-GHSD) was developed to solve the problems found in a static rack-type greenhouse solar dryer for drying fish. The experiments were carried out in four drying modes: mode 1 (MD1), mode 2 (MD2), mode 3 (MD3), and mode 4 (MD4); the performances of these modes were compared to each other. In MD1 and MD2, the RRT-GHSD was operated with exhaust air recycling at 100% and 50%, respectively, and heat recovery was utilized. MD3 and MD4 involved operating the RRT-GHSD with and without heat recovery, respectively, and without exhaust air recycling. The specific moisture evaporation rate (SMER) (0.223 kg/kWh) and efficiency of thermal dryer (39.16%) were found highest for MD1 and lowest for MD4. The specific consumption of energy (SEC) was found lowest (6.905 kW h/kg) for MD1 and highest for MD4. MD1 could save heat energy around 70.2%. The drying rate was found highest (4.79 kg/h) for MD1 and lowest for MD3. Furthermore, MD1 exhibited the highest exergy efficiency at 63.11%, surpassing MD2's 54.96%. Notably, RRT-GHSD not only ensures uniform air distribution but also maintains high drying product quality. The experimental moisture ratio (MR) data displayed an excellent relationship with the Page model.

Keywords Fish, rotating rack, rack-type, greenhouse solar dryer, air recirculation system, biomass furnace, performance.

1. Introduction

Indonesia, one of the world's largest fish-producing countries, achieved a significant fish production of 24.85 million tons in 2022. This production comprised 7.99 million tons from capture fisheries and 16.87 million tons from aquaculture. Notably, this total production represented a substantial increase of 13.63% when compared to the 2021 production, which stood at 21.87 million tons. Indonesia is also among the world's leading fish consumers, with a fish consumption rate of 56.48 kg per capita in 2022. This figure marked a 2.39% increase from the 2021 consumption rate, which was 55.16 kg per capita [1].

Fish is a widely consumed food ingredient cherished not only for its delectable taste but also for its numerous health benefits, owing to its rich content of vitamins A and D, along with essential minerals like, P_4O_{10}, Mg, Se, I, and Ca [2]. However, fish is a biologically active product prone to spoilage and decay, primarily due to its high moisture content, which promotes the rapid growth of microorganisms. Therefore, it is crucial to handle fish with precision, speed, and correctness to maintain its quality and prolong its shelf life before reaching the market. One effective method for preserving fish is through the process of drying, which entails utilizing heat energy to decrease the moisture content from the product (MC) to a predetermined level [3].

In tropical countries like Indonesia, the drying of biologically active products typically harnesses solar energy, given the consistent abundance of sunlight throughout the year, cheapness and cleanness [4-6]. This is primarily achieved through methods namely traditional drying and solar dryers. Traditional drying involves placing biologically active products directly under the sun, making it a simple and

economical method. However, it has drawbacks, including concerns about hygiene, lower product quality, and extended drying durations. On the other hand, solar dryers are a common option for drying biologically active products, with two common types being rack-type cabinet solar dryers (RT-CSD) and static rack-type greenhouse solar dryers (SRT-GHSD). These solar dryers offer more controlled and efficient drying processes compared to traditional drying.

Numerous sudies have explored the use of RT-CSD for drying of biologically active products, including fishery products such as channa, walking catfish climbing perch, swamp eel, and tilapia [7], and striped snakehead fish [8]; medicinal herbs such as onion slice [9], thymus and mint [10], red chilli [11], rosella [12], and *centella asiatica* L. [13]; fruits such as mango [14], and cabya [15]; vegetables such as mushroom [16], bitter gourd [17], and tomato [18]; food products such as copra [19].

A common observation in many of these studies is that RT-CSD offers hygienic and cost-effective drying. However, it is worth noting that RT-CSD is best suited for lower capacities, and differences in drying rates and final moisture content (MC) can occur between products on the bottom rack and the top rack. These variations may be due to differences in the heat energy received by the drying products, as well as differences in air temperature inside the dryer.

In a study, Prasad and Vijay [20] examined the distribution of air temperatures within a drying chamber of a RT-CSD during the drying of ginger and curcuma. The air temperatures on the bottom, middle, and top racks were found to be approximately 49.8 °C, 42.2 °C, and 39.9 °C, respectively. Furthermore, 15.59% was found to be the RT-CSD's thermal efficiency.

In a separate study, Mohanraj and Chandrasekar [21] examined the final MC of copra on the bottom and top racks within a drying chamber of a RT-CSD. The MC was found to be 7.8% (wb) on the bottom rack and 9.7% (wb) on the top rack after drying for 82 hours, starting with an initial MC of 51.8% (wb). Furthermore, it was determined that the RT-CSD's thermal efficiency was 24%.

In a subsequent study, Mallikarjuna et al. [22] performed an investigation on the distribution of air temperature, final moisture content (MC) of green chilies on each rack in the drying chamber, and the thermal efficiency of a RT-CSD. The air temperature within the dryer was found to be approximately 50.68 °C in rack 1, 49.75 °C in rack 2, 48.42 °C in rack 3, and 47.15 °C in rack 4. The final MC of green chilies in rack 1, rack 2, rack 3, and rack 4 were 0.0043, 0.0101, 0.0601, and 0.1278 kg/kg (db), respectively with an initial MC of approximately 8.3935 kg/kg (db). The thermal efficiency of RT-CSD was found to be 9.15%.

In a study conducted by Lingayat et al. [23], an inquiry was conducted to evaluate distribution of air temperature, drying rate of bananas for each rack in the drying chamber, and the rack-type cabinet solar dryer's (RT-CSD) thermal efficiency. The air temperature within the dryer was measured and found to be approximately 55 °C in rack 1, 51 °C in rack 2, and 47 °C in rack 3. The drying rate of bananas was observed to vary among the racks, with the bottom rack exhibiting a greater drying rate compared to the other racks. This difference is attributed to the fact that the product placed on the bottom rack receives more heat energy from the drying air, leading to faster drying. The thermal efficiency of the RT-CSD, as determined in this study, was found to be 17.73%.

Many sudies explored the use of SRT-GHSD for drying of biologically active products, including fishery products such as silver jew fish [24], salted catfish [25], and medium size queenfish [26]; medicinal herbs such as pepper and garlic [27], onion flakes [28], peppermint [29,30], chilli [31], wild ginger [32], java tea and sabah snake grass [33], red pepper [34], and cayenne pepper [35]; fruits such as grapes [36,37], and gooseberries [38]; vegetables such as cabbage and peas [39]; food products such as jaggery [40].

In many studies, the general consensus is that static rack-type greenhouse solar dryers (SRT-GHSD) are well-suited for large-capacity drying, offer hygienic conditions, and result in shorter drying times. However, these dryers have some disadvantages. They may experience reduced drying rates during periods of low solar irradiance, and the temperature distribution of the air within the drying chamber can be uneven. This uneven temperature distribution leads to variations in the heat energy received by the fish being dried, resulting in non-uniform moisture content (MC) in different racks. As a consequence, some fish may be dry, while others remain moist, leading to inconsistent product quality. Moreover, higher MC levels in some areas of the product can create favorable conditions for the growth of microorganisms or fungi, further compromising the dried fish's quality.

In a related study, Kaewkiew et al. [31] examined the distribution of air temperature at five distinct locations within the drying chamber of a SRT-GHSD used for drying chili. They observed variations in temperature at these different locations.

In a study conducted by Ratnawati [41], it was reported that the air temperatures on rack 1, rack 2, and rack 3 within the drying chamber of a SRT-GHSD used for drying *Eugenia caryophyllus* were recorded at 46.9 °C, 39.6 °C, and 38.0 °C, respectively.

In another study by Vijaykumar et al. [42], the distribution of air temperature within the drying chamber of a static rack-type tunnel solar dryer used for drying chilies was investigated. The study revealed that the temperature varied within the dryer, with temperatures ranging from 29 °C to 56 °C at the front, from 30.5 °C to 58.5 °C in the middle, and from 29.5 °C to 57.5 °C at the back.

In a later study by Aritesty and Wulandani [32], the distribution of air temperature, final MC of wild ginger on the upper (top), middle, and lower (bottom) racks within the drying chamber, and the performance of a SRT-GHSD were investigated. The air temperature was recorded as 53.10 °C, 44.81 °C, and 40.77 °C for the upper (top), middle, and lower (bottom) racks, respectively. The final MC of *Curcuma xanthorizza* Roxb was found to be 11.56%, 12.00%, and 11.45% (dry basis) for the upper (top), middle, and lower (bottom) racks, respectively. In addition, the dryer's thermal efficiency was 8% and its overall energy consumption was 29 MJ/kg.

The RT-CSD and SRT-GHSD, as previously discussed, come with certain disadvantages. In addition to the issues mentioned, these dryers also suffer from a low drying rate, making it challenging to achieve drying during periods of low solar radiation. Moreover, they result in substantial thermal energy loss through the exhaust air, as the air leaving the dryer is typically at a high temperature. This not only increases energy consumption within the drying system but also diminishes the overall drying system's performance.

In an attempt to minimize heat loss from the drying chamber's exhaust air, Sarsavadia [9] implemented an exhaust air recirculation system on an RT-CSD for drying onions. This innovation achieved significant energy savings, amounting to 70%, by recycling 90% of the exhaust air. This approach effectively minimized the loss of thermal energy and improved the drying process's energy efficiency.

Soponronnarit and Prachayawankorn [43] has equipped an exhaust air recirculation system on a fluidized bed dryer. It was discovered that recycling 80% of the exhaust air could result in an energy savings of up to 28%.

Darvishi et al. [44] investigated the effects of air recirculation on the amount of energy consumed and the exergy efficiency of a fluidized bed dryer (FBD) for drying sliced mushrooms. Without air recirculation, they discovered that the SEC and exergy efficiency in the range of 56.42-221.24 MJ/kg and 0.81%-3.94%, respectively. The SEC and exergy efficiency in the range of 14.73-43.14 MJ/kg and 10.40%-30.57%, respectively, with 100% air recirculation.

To address the challenge of maintaining the drying process under low sunlight conditions, Yahya [11] developed an innovative solution by integrating a biomass furnace with a single-stage heat exchanger into an RT-CSD for drying red chili. This integration allowed for the effective control of air temperature within the range of 68.4–71.8 °C, enabling continuous drying even in conditions of limited sunlight. According to the study, the solar collector and biomass furnace accounted for 14.7% and 37.8%, respectively, of the total energy required during the drying process. The SMER of 0.14 kg/kWh was attained on average, and the dryer's thermal efficiency reached to 9.03%.

In order to dry rice, Yahya et al. [45] evaluated the energy contributions and performance of an FBD using hybrid energy. Through the use of a biomass furnace, the air temperature could be elevated and effectively maintained within a range of 78.9-81.6 °C. Their findings revealed that the solar collector and biomass furnace made substantial contributions to the energy supply for the drying system, with a share of 11% and 30%, respectively. In the meantime, the dryer's thermal efficiency, SEC, exergy efficiency, and SMER were 15.4%, 4.76 kWh/kg, 41.3%, and 0.24 kg/kWh, respectively.

Hamdani et al. [26] conducted a study where they integrated a biomass furnace with a single-stage heat exchanger into a tunnel-type Static Rack-Type Greenhouse Solar Dryer (SRT-GHSD). This integration aimed to facilitate the drying process, particularly for medium-sized queenfish, even under conditions of low solar radiation. Their findings indicated that the heat energy generated from burning biomass fuels allowed the drying process to be carried out or continued effectively in low solar radiation conditions. Furthermore, they reported that the air temperature within the dryer could be maintained in the range of 40–50 °C from 16:00 to 06:00.

However, a biomass furnace utilizing a single-stage heat exchanger has a significant drawback: it results in substantial heat energy loss through the high-temperature flue gas from the chimney. This, in turn, increases energy consumption within the drying system and diminishes overall drying performance.

To solve the limitations of existing drying methods, considering the large amount of energy required in the drying process and the abundance of alternative energy sources (renewable energy sources such as solar energy and biomass energy) [46-48], innovation in drying technology is needed. The dryer is a rotary rack-type greenhouse solar dryer (RRT-GHSD) integrated with an air recirculation system and biomass furnace using a two-stage heat exchanger. And also, to our knowledge, the performance of this dryer for drying tilapia fish has not been studied. Thus, this study aimed to fabricate and investigate its performance.

2. Materials and Methods

2.1. Experimental Set-up

A rotary rack-type greenhouse solar dryer (RRT-GHSD) equipped with an air recirculation system and a biomass furnace using a two-stage heat exchanger was designed and fabricated for fish drying. The drying system comprises a greenhouse (drying chamber), racks, a rotary transmission system, a biomass furnace, an air distributor, an air recirculation system, air ducts, and a blower, as presented in Figs. 1. The greenhouse measures 2.0 meters in width, 2.5 meters in height, and 6.5 meters in length, covered with a 5 mm-thick transparent glass plate. The biomass furnace features a two-stage heat exchanger, with the first stage serving as the primary air heater and the second stage functioning as an air preheater (heat recovery). Each heat exchanger consists of 14 pipes with a 2.5-inch diameter, constructed from mild steel material. The rotary transmission system includes a 5 HP, 1420 rpm electric motor, a gearbox with a gear ratio of 1:50, and two sprockets—one with 16 teeth and the other with 23 teeth, linked by a roller chain. The air distributor is equipped with guide blades to ensure uniform airflow into the drying chamber. Both the air distributor, air recirculation system, and air ducts are insulated with thermal insulation material (fiber glass) to minimize heat loss. The racks are sized at 0.5 meters in width and 0.6 meters in length, constructed from aluminum strips and steel wire mesh. A total of 60 racks are used in the system. A centrifugal blower is used in the drying chamber to circulate drying air, with an electric power rating of 3.7 kW.

(a)

(b)

Figs. 1. Photographs of the RRT-GHSD equipped with an air recirculation system and a biomass furnace using heat recovery: (a) front view and (b) back view.

2.2. Experimental Procedure

Four distinct operation modes were used for the drying studies. In MD1 and MD2, the drying system recycled 100% and 50% of the exhaust air, respectively, while employing heat recovery (second-stage heat exchanger) on the biomass furnace. In MD3 and MD4, the system operated both with and without heat recovery (second-stage heat exchanger), respectively, and without recycling the exhaust air. The reason for choosing to use air 100% comes from the exhaust air of the drying system and 0% from the environment for the drying process in MD1, and 50% comes from the exhaust air of the drying system and 50% from the environment in MD2 is because these values have quite a big difference and make it easy to see the effect on energy consumption and dryer performance. A schematic of a rotary rack-type greenhouse solar dryer equipped with an air recirculation system and a biomass furnace using heat recovery is provided in Fig. 2, and operating modes 1-4 are depicted in Figs. 3. Fresh Tilapia fish was procured from ocal fish breeders in Padang. The fish were cleaned, gutted, and halved as shown in Fig 4 (a). After thorough cleaning and weeding, approximately 90 kg of fish was loaded into the drying chamber, where it was secured using racks, as can be seen in Fig 4 (b). The initial MC of the tilapia fish were conducted by using the oven method at 105 ± 3 °C. During the drying experiments, the ambient temperature, the air temperature at inlet, inside and outlet of drying chamber, and the air temperature at inlet and outlet of biomass furnace were measured by using thermocouples (type: T; range: -200 to 400°C; accuracy: $\pm 0.1\,^{\circ}C$; made in: Japan). The solar irradiance was measured by using pyranometer (type: LI-200; range: $0 - 2000$ Wm^{-2}; accuracy: ± 0.1 Wm^{-2}; made in: Japan). An anemometer was used to measure the air velocity (type: HT-383; range: $0 - 30$ ms^{-1}; accuracy: ± 0.2 ms^{-1}; made in: China). The temperature and solar irradiance were recorded by data logger (type: AH4000; accuracy: $\pm 0.1\,^{\circ}C$; made in: Japan). A weighing scale (type: Camry; accuracy: ± 0.1 kg; made in: China) was used to determine the weight of the fish. A weighing scale (type: CTG 602; range: $0 - 600$ gm; accuracy: ± 0.01g; made in: Japan) was used to determine the sample's weight loss. The biomass fuels use coconut shell charcoal. Rack rotation speed of 17 rpm. Sample weight loss was weighed, and measurements of solar irradiance and air temperature were made every 60 minutes.

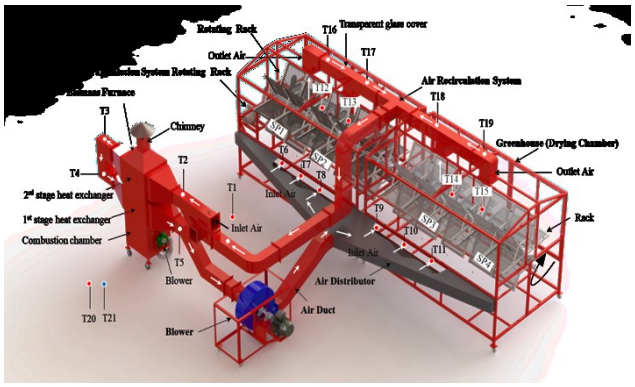

Fig. 2. Schematic of the RRT-GHSD equipped with an air recirculation system and a biomass furnace using heat recovery.

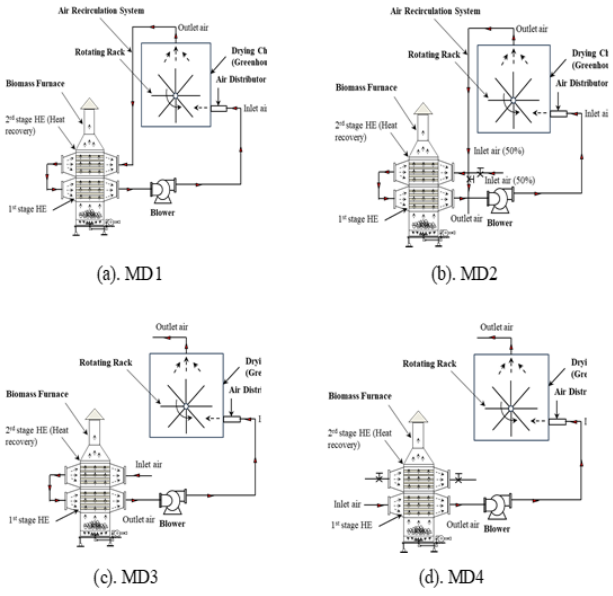

Figs. 3. Operating modes of the drying sysyem: (a) MD1, (b) MD2, (c) Md3, and (d) MD4.

Fig. 4 (a). The tilapia fish prepared for the drying experiment.

Fig. 4(b). The tilapia fish clamped with racks in the drying chamber.

The uncertainty was determined using the following formula [49,50]:

$$W_R = \left[\left(\frac{\partial R}{\partial x_1} w_1\right)^2 + \left(\frac{\partial R}{\partial x_2}\right) + \cdots + \left(\frac{\partial R}{\partial x_n} w_n\right)^2\right]^{1/2} \quad (1)$$

2.3. Analyses of Drying Characteristics and Performance

The drying characteristics for tilapia, the performance of the RRT-GHSD equipped with an air recirculation system and a biomass furnace using heat recovery were calculated using the equations in Table 1.

Table 1. The equations employed to calculate the drying kinetic and performance of the RRT-GHSD

Parameter	Formula	Eq.no.	Ref.
Drying kinetic			
Fish moisture content (db)	$M_{dbf} = \frac{m_{wetf} - m_{df}}{m_{df}}$	(2)	[3]
Fish moisture content (wb)	$M_{wbf} = \frac{m_{wetf} - m_{df}}{m_{wetf}}$	(3)	[3]
Drying rate (DR)	$DR = \dot{m}_{water} = \frac{M_{dbf,t+dt} - M_{dbf,t}}{dt}$	(4)	[56]
Moisture ratio	$MR = \frac{M_t}{M_o}$	(5)	[56]
Newton model	$MR = \exp(-kt)$	(6)	[51,52]
Henderson and Pabis model	$MR = a\exp(-kt)$	(7)	[51,52]
Page model	$MR = \exp(-kt^n)$	(8)	[51,52]
The mean bias error	$MBE = \frac{1}{N}\sum_{i=1}^{N}(MR_{pre,i} - MR_{exp,i})^2$	(9)	[51,52]
The root-mean-square error	$RMSE = \left[\frac{1}{N}\sum_{i=1}^{N}(MR_{pre,i} - MR_{exp,i})^2\right]^{1/2}$	(10)	[51,52]
Performance of dryer			
Specific energy consumption	$SEC = \frac{Q_{lse} + Q_{lbmf} + W_{Mts} + W_{Bdr} + W_{Bbf}}{\dot{m}_{water}}$	(11)	[53]
Total electrical energy	$W_{Mt} = W_{Mts} + W_{Bdr} + W_{Bbf}$	(12)	[53]
Contribution of biomass fuel energy	$CE_{BF} = \frac{Q_{lbmf}}{Q_{lse} + Q_{lbmf} + W_{Mts} + W_{Bdr} + W_{Bbf}} \times 100\%$	(13)	[54]
Contribution of solar energy	$CE_{SE} = \frac{Q_{lse}}{Q_{lse} + Q_{lbmf} + W_{Mts} + W_{Bdr} + W_{Bbf}} \times 100\%$	(14)	[45,53]
Specific moisture extraction rate	$SMER = \frac{\dot{m}_{water}}{Q_{lse} + Q_{lbmf} + W_{Mts} + W_{Bdr} + W_{Bbf}}$	(15)	[16]

Thermal dryer efficiency	$\eta_{th} = \frac{m_{water} H_{fg}}{Q_{Ise} + Q_{Ibmf} + W_{Mts} + W_{Bdr} + W_{Bbf}}$	(16)	[11,55]
Exergy efficiency of greenhouse	$\eta_{Ex} = \frac{Ex_{GHi} - Ex_{loss}}{Ex_{GHi}} = 1 - \frac{Ex_{loss}}{Ex_{GHi}}$	(17)	[54]
Exergy losses of greenhouse	$Ex_{loss} = Ex_{GHi} - Ex_{GHo}$	(18)	[54]
Exergy input into the greenhouse	$Ex_{GHi} = \dot{m}_{da} C_{Pda} \left[(T_{i,GH} - T_{amb}) - T_{amb} \ln \frac{T_{i,GH}}{T_{amb}} \right]$	(19)	[54]
Exergy output for greenhouse	$Ex_{GHo} = \dot{m}_{da} C_{Pda} \left[(T_{o,GH} - T_{amb}) - T_{amb} \ln \frac{T_{o,GH}}{T_{amb}} \right]$	(20)	[54]
Solar energy input	$Q_{Ise} = I_T A_{SC}$	(21)	[55]
Power input of blower biomass furnace	$W_{Bbf} = VI \cos\varphi$	(22)	[45,54]
Power input of dryer blower	$W_{Bdr} = \sqrt{3} VI \cos\varphi$	(23)	[45]
Power input of transmission system motor	$W_{Mts} = \sqrt{3} VI \cos\varphi$	(24)	[45]
Heat energy input of biomass furnace	$Q_{Ibmf} = \dot{m}_{bf} CV_{bf}$	(25)	[54]

3. Results and Discussion

The uncertainties of measurement of the air temperature, solar irradiance, air velocity, weight of fish, weight of biomass of fuel, and measurement of time were found to be ± 0.17 ℃, ± 0.14 W/m^2, ± 0.24 m/s, $\pm$ 0.14 kg, $\pm$ 0.11kg, and ± 0.1 min, respectively.

In RRT-GHSD, the quality of the drying products, or the uniformity of the final MC of the fish is primarily influenced by the even distribution of hot air within the drying. The variation in air temperature at different positions inside the drying chamber (T12, T13, T14, and T15) for various drying modes over time is shown in Figs 5. The graphs illustrate that these temperatures for each mode (MD1, MD2, MD3, and MD4) tend to converge over time. This uniformity is achieved due to the rotational effect of the racks, ensuring uniform air distribution within the drying chamber.

The air temperature within the drying chamber or greenhouse is influenced by two main factors: the intensity of sunlight received by the greenhouse (drying chamber) and the temperature of the incoming air (heated by the biomass furnace) into the drying chamber. Specifically, higher sunlight intensity and warmer incoming air result in higher air temperatures within the drying chamber. The variation in solar irradiance and air temperature within the drying chamber (drying air temperature) during the drying operations of MD1, MD2, MD3, and MD4 over time is presented in Fig 6. The weather conditions during each drying mode were consistently sunny, with recorded solar radiation ranging from 217.0 to 801.6 W/m², 184.9 to 787.5 W/m², 224.3 to 780.7 W/m², and 386.5 to 782.8 W/m² for MD1, MD2, MD3, and MD4, respectively. The respective average values were 633.4, 477.2, 573.0, and 645.9 W/m². Meanwhile, the recorded drying air temperatures during the drying operations of MD1, MD2, MD3, and MD4 fell within the ranges of 53.0-62.5 °C, 47.0-60.7 °C, 51.9-61.8 °C, and 53.0-63.1 °C, with average values of 57.6 °C, 54.9 °C, 58.1 °C, and 58.0 °C, respectively.

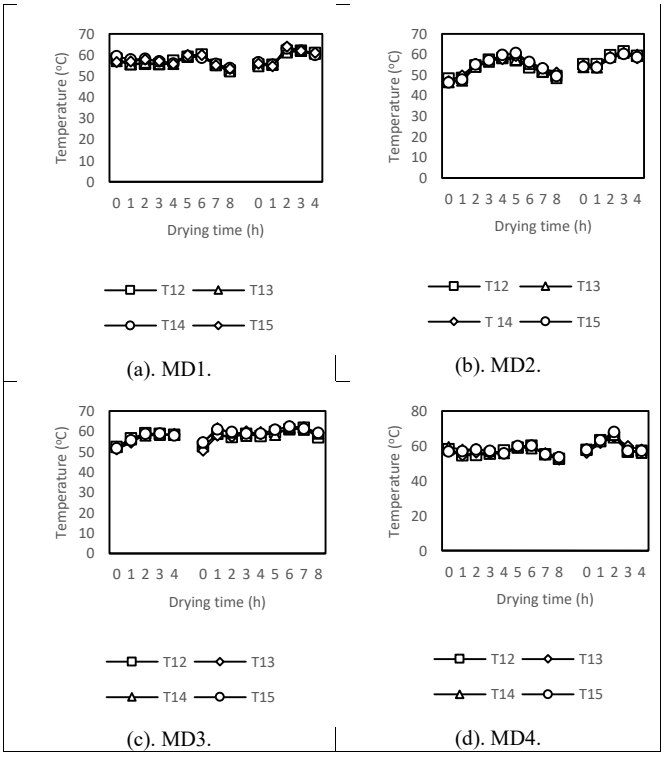

Figs. 5. Variation in the air temperature for different positions and for different drying modes at the inside of drying chamber vs time.

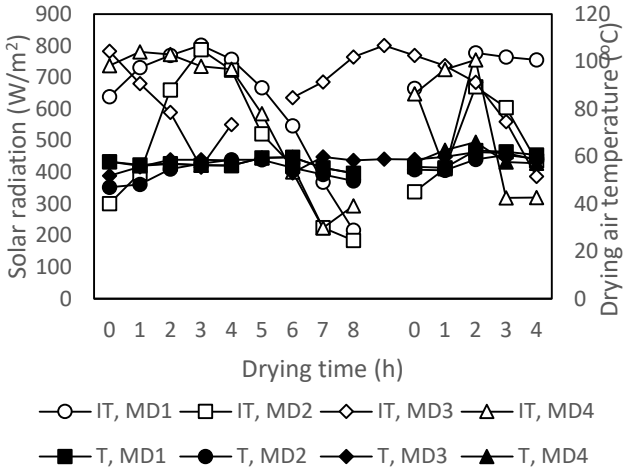

Fig. 6. Variation in solar irradiance and drying air temperature vs time.

The time required, change in material weight, and the quantity of energy consumed in the drying process are dependent on several key factors, including the initial and final MC of the material, the quantity of material, the drying air temperature, the velocity of air, the surface area of the material, and the material thickness. The variations in fish weight change and MC of the fish over time for different drying modes are illustrated in Fig 7 and Fig 8. The drying time for each mode was as follows: MD1 (9.89 hours), MD3 (10.25 hours), MD2 (11.27 hours), and MD4 (12 hours). The initial weights of the fish were 90.56 kg (with an initial MC of 2.234 g/g db or 69.08% wb), 91.46 kg (with an initial MC of 2.267 g/g db or 69.40% wb), 89.20 kg (with an initial MC of 2.186 g/g db or 68.81% wb), and 89.94 kg (with an initial MC of 2.212 g/g db or 68.87% wb) for MD1, MD2, MD3, and MD4, respectively. The final weight was 35.04 kg with a final MC of 0.251 g/g db or 20% wb under a mass flow rate of 0.45 kg/s. The average drying air temperatures were 57.6 °C for MD1, 54.9 °C for MD2, 58.1°C for MD3, and 59.0 °C for MD4. In terms of energy consumption, MD1 required the least energy (208.7 kW), followed by MD2 (299.9 kW), MD3 (352.9 kW), and MD4, which required the highest energy (537.8 kW).

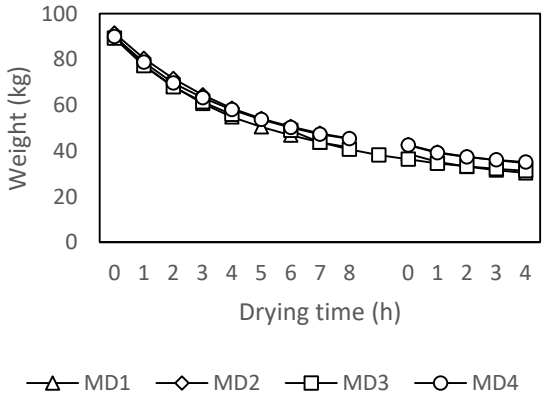

Fig. 7. Variation in weight change of fish vs time.

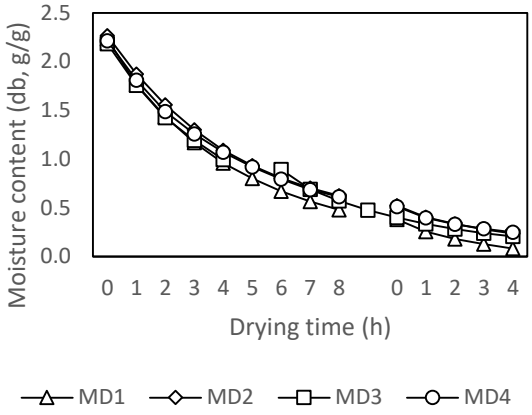

Fig. 8. Variation in MC of fish vs time.

The drying rate (DR) of a material is a critical factor influencing the time required for drying. It depends on the driving force for the mass transfer of water within the material to its surface or the rate of water evaporation into the surrounding environment. In essence, a higher driving force for mass transfer or a faster rate of water evaporation corresponds to a higher DR for the material. Fig. 9 illustrates the variation of the DR with drying time for different drying modes. The highest DR for fish was achieved in MD1, primarily due to its high rate of water evaporation. The drying rates for fish in MD1, MD2, MD3, and MD4 ranged from 1.25 to 13.21 kg/h, 1.19 to 11.08 kg/h, 0.86 to 12.02 kg/h, and 1.02 to 11.24 kg/h, respectively. The respective average values were 4.79, 4.50, 4.26, and 4.34 kg/h.

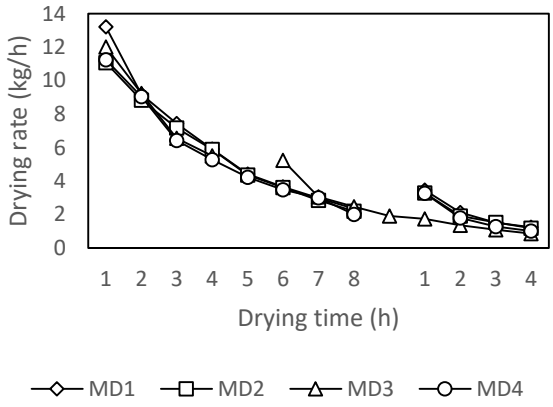

Fig. 9. Variation in DR fish with drying time.

During the drying processes, it is desirable to achieve minimal energy usage (the total input of energy) in the drying system, while still drying large quantities of material at a high drying rate or within a short drying time. In the RRT-GHSD, energy is derived from two sources: heat energy, employed to heat the drying air, and electric energy, employed to power the blower and motor. Fig 10 presents the variation of SEC with drying time for various drying modes. SEC is influenced by both the total input of energy of the drying system required for drying the fish and the drying rate, which is the rate at which water evaporates. The lowest SEC was achieved in MD1, primarily due to its low energy consumption and high drying rate. SEC values in MD1, MD2, MD3, and MD4 fell within

the ranges of 1.69-17.57 kWh/kg, 2.39-21.35 kWh/kg, 3.15-35.66 kWh/kg, and 3.95-46.38 kWh/kg, respectively, with respective average values of 6.91, 9.14, 15.0, and 17.3 kWh/kg.

Changes in SMER as a function of drying time for various drying modes is depicted in Fig 11. SMER depends on the drying rate, which signifies the rate at which water evaporates, and the energy consumed (the total input of energy) by the drying system to dry the fish. In simple terms, a high drying rate and low energy consumption by the drying system correspond to a high SMER. The highest SMER was achieved in MD1, primarily due to its high drying rate and low energy consumption. SMER values in MD1, MD2, MD3, and MD4 ranged from 0.057 to 0.59 kg/kWh, 0.05 to 0.42 kg/kWh, 0.03 to 0.32 kg/kWh, and 0.02 to 0.25 kg/kWh, respectively, with average values of 0.22, 0.16, 0.12, and 0.10 kg/kWh.

Changes in thermal dryer efficiency as a function of drying time for various drying modes is displayed in Fig 12. Thermal dryer efficiency depends on the drying rate of the fish, air temperature, and the energy consumed by the drying system. In simple terms, a high drying rate, high air temperature, and low energy consumption by the drying system correspond to a high thermal dryer efficiency. The highest average thermal dryer efficiency was achieved in MD1 (14.74%), followed by MD2 (10.77%), MD3 (7.87%), and MD4 (6.52%). The range of thermal dryer efficiency is displayed as follows: 3.77% to 39.16% for MD1, 3.10% to 27.63% for MD2, 1.86% to 21.04% for MD3, and 1.43% to 16.76% for MD4.

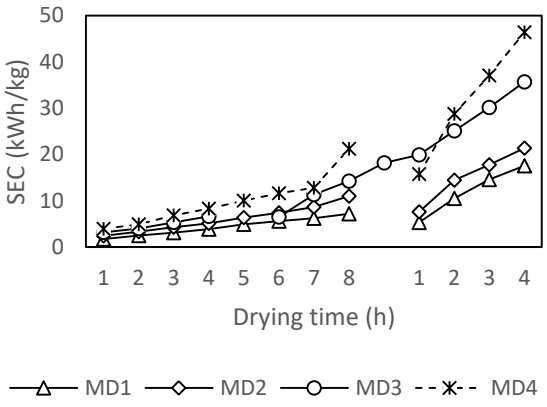

Fig. 10. Variation in SEC vs time.

The variation of exergy efficiency with drying time for various drying modes is displayed in Fig. 13. The value of exergy efficiency is notably impacted by the temperature of the drying air, with lower drying air temperatures corresponding to lower exergy efficiency. The lowest exergy efficiency was observed in MD2 (54.96%) due to the low drying air temperature (54.9 °C). Exergy efficiency values in MD1, MD2, MD3, and MD4 ranged from 40.65% to 76.33%, 36.11% to 73.43%, 57.63% to 96.38%, and 63.55% to 92.12%, respectively, with average values of 63.11%, 54.96%, 79.07%, and 80.34%.

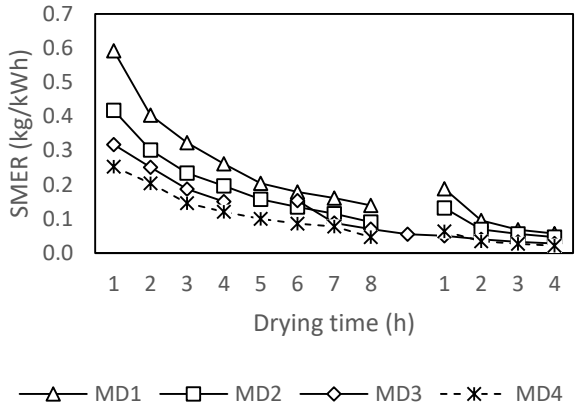

Fig. 11. Variation in SMER vs time.

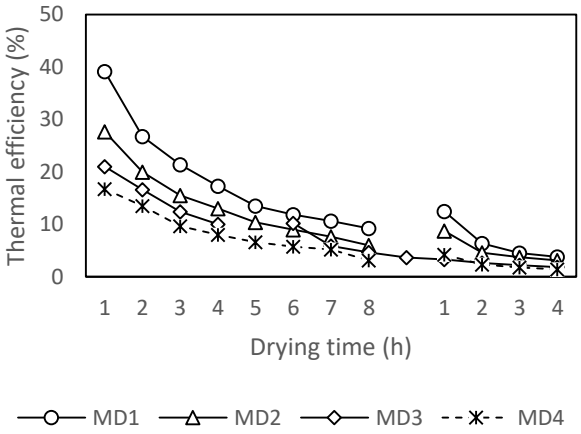

Fig. 12. Variation in thermal dryer efficiency vs time.

The variation of solar energy and biomass fuel energy supplied (input) to the drying system with drying time for various drying modes is displayed in Fig. 14. In MD1, MD2, MD3, and MD4, the solar energy input to the dryer ranged from 2.28 kW to 8.42 kW, 1.94 kW to 8.27 kW, 4.06 kW to 8.41 kW, and 2.23 kW to 8.20 kW, respectively, with average values of 6.62 kW, 5.29 kW, 6.67 kW, and 5.74 kW. The total solar energy supplied to the drying system was 79.413 kW, 63.43 kW, 80.06 kW, and 68.84 kW, respectively. Meanwhile, the biomass fuel energy supplied to the drying system in MD1, MD2, MD3, and MD4 ranged from 8.83 kW to 13.25 kW, 8.83 kW to 30.92 kW, 17.67 kW to 30.92 kW, and 22.08 kW to 44.16 kW, respectively, with average values of 10.31 kW, 18.03 kW, 23.99 kW, and 34.60 kW. The total biomass fuel energy supplied to the drying system was 123.66 kW, 216.41 kW, 287.07 kW, and 415.15 kW, respectively.

The variation of contribution of solar energy (CSE) to the dryer with drying time for various drying modes is displayed in Fig 15. The highest CSE was observed in mode 1 (31.06%) due to the low consumption of biomass fuel energy and the total energy consumed in the drying system. CSE to the drying system in MD1, MD2, MD3, and MD4 ranged from 11.58% to 38.60%, 8.25% to 38.91%, 11.69% to 27.83%, and 6.29% to 18.79%, respectively, with average values of 31.06%, 19.95%, 19.85%, and 12.68%.

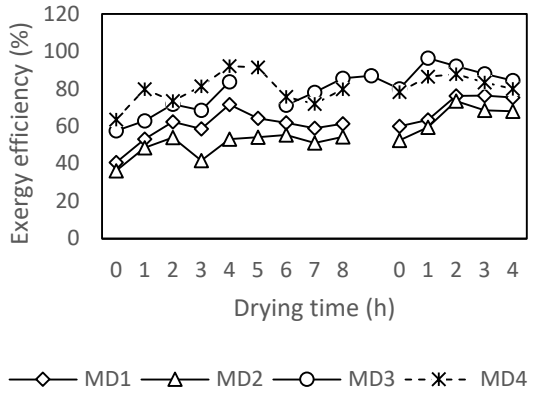

Fig. 13. Variation in exergy efficiency vs time.

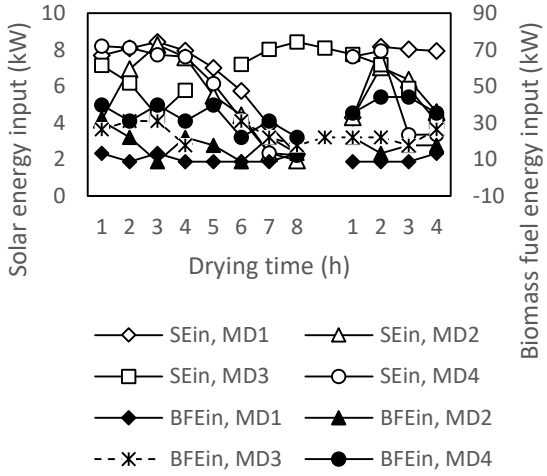

Fig. 14. Variation in solar energy and biomass fuel energy supplied with drying time.

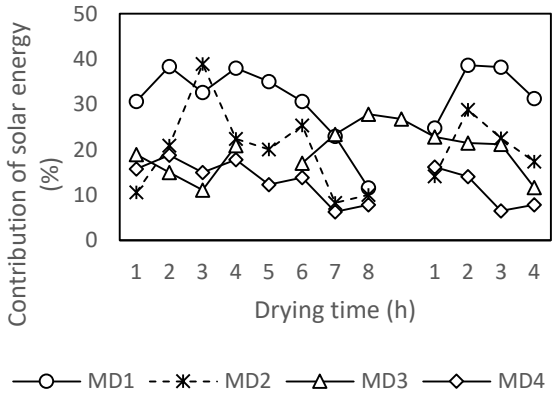

Fig. 15. Variation in contribution of solar energy to the drying system vs time.

The variation of contribution of biomass fuel energy (CBFE) to the dryer with drying time for various drying modes is persented in Fig 16. The highest CBFE was observed in MD4 (77.58%) due to the high total energy consumption in the drying system. CBFE to the drying system in MD1, MD2, MD3, and MD4 ranged from 41.77% to 67.33%, 41.56% to 78.80%, 58.44% to 78.40%, and 71.60% to 85.48%, respectively, with average values of 48.89%, 64.14%, 69.00%, and 77.58%.

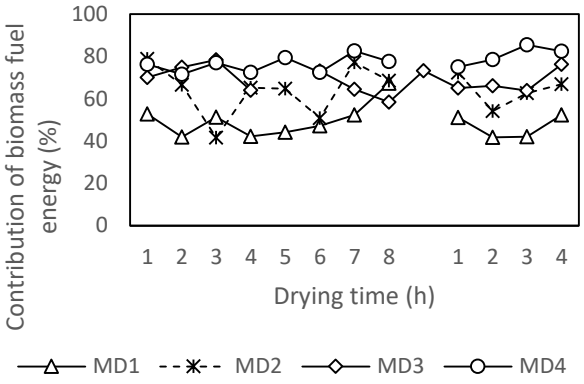

Fig. 16. Variation in the contribution of biomass fuel energy to the drying system with drying time.

The experimental results of RRT-GHSD performance are presented in Table 2.

Table 2. Evaluation of the RRT-GHSD performance

Parameters	Unit	Values			
		Mode	Mode	Mode	Mode 4
Initial weight	kg	90.56	91.49	89.20	89.94
Final weight	kg	35.04	35.04	35.04	35.04
Initial MC (wb)	%	69.08	69.40	68.81	68.87
Final MC (wb)	%	20	20	20	20
Initial MC (db)	g/g	2.234	2.267	2.186	2.212
Final MC (db)	g/g	0.251	0.251	0.251	0.251
Ave. drying air temperature	°C	57.64	54.89	58.10	57.96
Drying time	h	9.89	11.27	10.25	12
Ave. drying rate (DR)	kg/h	4.79	4.50	4.26	4.34
Ave. SMER	kg/kWh	0.22	0.16	0.12	0.10
Ave. SEC	kW h/kg	6.91	9.14	15.00	17.29
Ave. STEC	kW h/kg	5.53	7.70	13.15	15.72
Ave. SEEC	kW h/kg	1.37	1.43	1.85	1.57
Thermal efficiency of the dryer	%	39.16	27.63	21.04	16.76
Ave. exergy efficiency	%	63.11	54.96	79.07	80.34
Ave. improvement potential	W	141.75	204.85	52.95	38.37
Ave. efficiency of biomass furnace	%	55.36	55.29	54.94	41.03
Ave. solar energy input	kW	6.62	5.29	6.67	5.74
Ave. biomass fuel energy input	kW	10.31	18.03	23.92	34.60

Different materials exhibit varying drying kinetics, and their drying behavior is influenced by their specific characteristics. Drying kinetics serve as a means to describe this behavior, typically represented in the form of changes in moisture ratio (MR) over time. These drying behaviors can be effectively described through mathematical models, often referred to as drying models. To establish a drying model, a

process known as curve fitting is employed. This involves fitting the MR data over time to various drying mathematical models, followed by a non-linear regression analysis to identify the most suitable and accurate drying model equation based on experimental results. The accuracy of the model is assessed using key indicators namely the coefficient of determination (R^2), mean bias error (MBE), and root mean-square error (RMSE), where high R^2 and MBE values, along with low RMSE values, indicate a high level of accuracy.

In this research, the drying behavior of fish in the RRT-GHSD under different drying modes was fitted to three drying models: the Newton model, Page model, and Henderson-Pabis model. The table below (Table 3) provides the regression constants and the values of R^2, MBE, and RMSE for these drying models. Among the three mathematical models, the Page model stands out as the most appropriate and accurate choice for describing fish drying behavior. This conclusion is based on its highest R^2 and MBE values and the lowest RMSE values when compared to other models for each drying mode.

Table 3. Statistics from drying curve mathematical modelling

Model	Mode	Coefficients			R^2	MBE	RMSE
		a	k	n			
Newton	1		0.223		0.9946	0.00067	0.02600
	2		0.171		0.9978	0.00023	0.01529
	3		0.186		0.9981	0.00139	0.03729
	4		0.169		0.9972	0.00034	0.01843
Henderson and Pabis	1	1.1143	0.2354		0.9745	0.00241	0.04911
	2	1.0184	0.1696		0.9970	0.00055	0.02344
	3	1.0446	0.1816		0.9986	0.00171	0.04140
	4	1.0373	0.1649		0.9971	0.00160	0.04010
Page	1		0.9942	0.2177	0.9877	0.00041	0.02028
	2		0.9455	0.1928	0.9981	9.86E-05	0.00993
	3		0.9298	0.2178	0.9986	8.03E-05	0.00896
	4		0.9173	0.2024	0.9979	9.81E-05	0.00990

The accuracy of experimental Moisture Ratio (MR) compared to MR predicted from the Page model in MD1, MD2, MD3, and MD4 is illustrated in Fig 17. This data shows that the model is appropriate for explaining fish drying behavior. This Page model can be used to design a rotary rack-type greenhouse solar dryer (RRT-GHSD) for drying tilapia fish according to the required drying capacity.

Fig 18 illustrates the variation of Drying Rate (DR) with Moisture Content (MC) of fish for different drying operation modes. These drying curves are instrumental in identifying distinct periods of fish drying rates. Notably, the drying curve reveals that fish does not exhibit a constant drying rate. This phenomenon is attributed to the absence of free water on the surface of the fish at the beginning of the drying process. During this stage, only a falling rate period is observed, and it is influenced by the movement of water from within the material to the surface. It is important to note that MC significantly affects the drying rate, greater MC leading to a greater rate of drying. From the drying curve, the regression equations were obtained for different drying mode as follow: for MD1: $DR = 0.2644 + 6.398\ (MC)$ and $R^2 = 0.9296$; for MD2: $DR = -0.4127 + 5.8104\ (MC)$ and $R^2 = 0.9533$; for MD3: $DR = -0.6473 + 6.8621\ (MC)$ and $R^2 = 0.9769$, and for MD4: $DR = -0.7202 + 6.1279\ (MC)$ and $R^2 = 0.9392$. These equations of DR can be used to predict drying times.

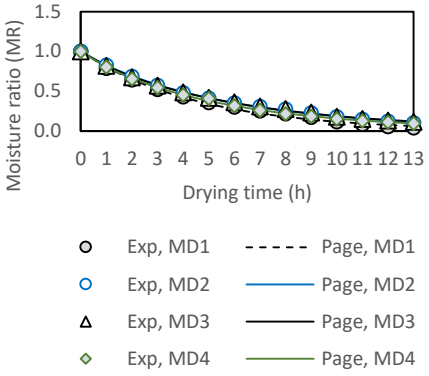

Fig. 17. Variation in MR of dried fish in MD1, MD2, MD3, and MD4 and page model vs time.

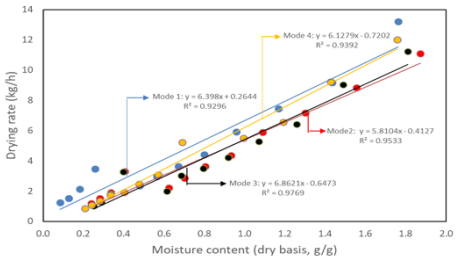

Fig. 18. Variation in DR with MC (db, g/g).

Figs 19 display the color of the fish samples both before drying and after being dried using the RRT-GHSD. As evident from the figure, the color of the fish after drying appears as a bright yellow. This observation suggests that the dried goods are of rather high quality.

(a). Before drying b). After drying

Figs. 19. Color of fish before and after drying.

The experimental results of drying tilapia fish using a rotary rack-type greenhouse solar dryer (RRT-GHSD: MD1) were compared with several types of dryers in references shown in Table 4, and Table revealed that this dryer (RRT-GHSD: MD1) is better than several types of dryers in the references. This is because the performance of the dryer is higher than that of several types of dryers in the references. Also, the distribution of air temperature and final moisture content of tilapia fish in the drying chamber was uniform.

Table 4. Experimental results of RRT-GHSD for tilapia fish drying in comparison with several dryers reported in the references

No	Dryer type	Drying products	Initial moisture content (%wb)	Time (h)	Distribution of air temperature in drying chamber	Final moisture content in drying chamber	ACR (%)	ES (%)	Energy contribution (%)		SMER (kg/kWh)	SEC (kWh/kg)	Efficiency (%)		Refs.
									CSE	CBFE			η_{th}	η_{Ex}	
1	Static rack-type cabinet solar dryer	Ginger	-	-	Not uniform	-	-	-	-	-	-	-	16	-	[20]
2	Static rack-type cabinet solar dryer	Copra	51.8	82	-	Not uniform	-	-	-	-	-	-	24	-	[21]
3	Static rack-type cabinet solar dryer	Green chili	8.4 db	-	Not uniform	Not uniform	-	-	-	-	-	-	9	-	[22]
4	Static-type cabinet solar dryer	Banana	-	-	-	-	-	-	-	-	-	-	18	-	[23]
5	Static rack-type greenhouse solar dryer	Eugenia caryophyllus	-	-	Not uniform	-	-	-	-	-	-	-	-	-	[41]
6	Static rack-type tunnel solar dryer	chili	-	-	Not uniform	-	-	-	-	-	-	-	-	-	[42]
7	Static rack-type greenhouse solar dryer	Wild ginger	-	-	Not uniform	Not uniform	-	-	-	-	-	-	8	-	[32]
8	Static rack-type cabinet solar dryer equipped with air recirculation system	Onion	86	5	-	-	90	70	22-41	-	-	-	-	-	[9]
9	Fluidized bed dryer equipped with air recirculation system	Paddy	38.5 db	-	-	-	80	20	-	-	-	-	-	-	[43]
10	Static rack-type cabinet solar dryer equipped with biomass furnace with single-stage heat exchanger	Red chili	-	-	-	-	-	-	14.7	37	0.14	-	9	-	[11]
11	Fluidized bed dryer equipped with biomass furnace with single-stage heat exchanger	Paddy	-	-	-	-	-	-	11	30	0.24	4.8	15	41	[45]
12	Rotary rack-type greenhouse solar dryer (RRT-GHSD: MD1)	Tilapia fish	69	9.89	Uniform	Uniform (20% wb)	100	70	12-37	42-67	0.22	6.9	39	63	Present study

ACR: air recirculation ratio; CBFE: contibution of biomass fuel energy; CSE: contribution of solar energy; ES: energy savings; SEC: specific energy consumption; SMER: specific moisture extraction rate; η_{Ex} : exergy efficiency for drying chamber; η_{th} : thermal dryer efficiency.

4. Conclusion

A novel RRT-GHSD designed for drying fish was tested and evaluated in this study. The experiments were conducted in four distinct drying modes, denoted as MD1, MD2, MD3, and MD4, and their performance was compared. In MD1 and MD2, the RRT-GHSD was operated with 100% and 50% recycling of exhaust air, respectively, and featured heat recovery. For MD3 and MD4, the RRT-GHSD was operated with and without heat recovery, respectively, without recycling exhaust air.

The results of these experiments are provided below.

- MD1, MD2, MD3 and MD4 reduced the MC of fish from 2.234 g/g db (69.08% wb), 2.267 g/g db (69.40% wb), 2.186 g/g db (68.81% wb) and 2.212 g/g db (68.87% wb), respectively to 0.251g/g db (20% wb) in 9.89 h, 11.27 h, 10.25h and 12h, respectively with a 0.45 kg/s mass flow rate, and average temperatures of 57.6 °C, 54.9 °C, 58.1 °C and 58.0 °C, respectively.
- The total energy consumed for drying fish in MD1 was the lowest (208.74 kW), followed by MD2 (299.9 kW), MD3 (352.9 kW), and MD4 (537.8 kW).
- The DR value was highest for MD1. The average values of DR of fish for MD1, MD2, MD3 and MD4 were 4.79, 4.50, 4.26, and 4.34 kg/h, respectively.
- The SMER in MD1 was the highest (0.22 kg/kWh), followed by those in MD2 (0.16 kg/kWh), MD3 (0.12 kg/kWh) and MD4 (0.10 kg/kWh).
- The SEC value in MD1 was the lowest (6.91 kWh/kg), followed by those in MD2 (9.14 kWh/kg), MD3 (15.00 kWh/kg), and MD4 (17.29 kWh/kg).
- The thermal dryer efficiency of MD1 was better compared to other modes. Those for MD1, MD2, MD3 and MD4 were 39.16%, 27.63%, 21.04% and 16.76%, respectively.
- The lowest exergy efficiency was obtained in MD2 (54.96%) due to low the drying air temperature (54.9 °C).
- The values of contribution of solar energy (CSE) to drying system in MD1, MD2, MD3 and MD4 were 31.06, 19.95, 19.85 and 12.68%, respectively.
- The values of contribution of biomass fuel energy (CBFE) to drying system in MD1, MD2, MD3 and MD4 were 48.89, 64.14, 69.00 and 77.58%, respectively.
- The values of biomass furnace efficiency in MD1, MD2, MD3 and MD4 were 55.36, 55.29, 54.94 and 41.03%, respectively.
- The experimental MR data displayed an excellent relationship with the Page model.

- The results indicated that in performance, MD1 was better than MD2, MD3 and MD4 because the $\dot{m}_{water}$, SMER, η_{th} and η_{Pickup} values were higher and the SEC value was lower.

Nomenclature

A_{GH}	solar greenhoure area (m^2)
Ave	average
C_a	air specific heat ($Jkg^{-1}°C^{-1}$)
C_{da}	drying air specific heat ($Jkg^{-1}°C^{-1}$)
CE_{BF}	contribution of biomass fuel energy (%)
CE_{SE}	contribution of solar energy (%)
CV_{bf}	caloric value for biomass fuel (kcal/kg)
Ex_{GHi}	exergy input into the greenhouse (J/s)
Ex_{GHo}	exergy output for greenhouse (J/s)
H_{fg}	the water vaporization's latent heat (kJ/kg)
I	current (A)
I_T	solar irradiance (W/m^2)
$\dot{m}_a$	mass flow rate of air (kg/s)
$\dot{m}_{bf}$	rate of consumption of biomass fuel (kg/s)
$\dot{m}_{da}$	drying air mass flow rate (kg/s)
$M_{dbf,t}$	moisture content of fish (db) at "t+Δt"
$M_{dbf,t+\Delta t}$	moisture content of fish (db) at "t"
MD	mode
m_{df}	mass of fish bone-dry (kg)
$\dot{m}_{water}$	drying rate (kg/min)
m_{wetf}	mass of wet fish (kg)
Q_{Ibmf}	heat energy input of biomass fuel (W)
Q_{Ise}	solar energy input (W)
SEC	specific consumption of energy (kWh/kg)
SMER	specific moisture extraction rate (kg/kWh)
T	temperature (°C)
T20&T21	dry bulk and wet bulk ambient temperature, respectively (°C)
t	time (min)
V	voltage (V)
W_{Bbf}	blower biomass furnace power input (W)
W_{Bdr}	dryer blower power input (W)
W_{Mts}	transmission system motor power input (W)
$\cos\varphi$	power factor
η_{Ex}	exergy efficiency of greenhouse (%)
η_{th}	thermal efficiency of dryer (%)
db	dry basis
wb	wet basis

Acknowledgments

The writers express gratitude to Kemdikbudristek of Indonesia for research funding through the "Penelitian Terapan Jalur Hilirisasi (PTJH)" project No.002/27.O10.5/PN/VII/2023.

Author Contributions

M. Yahya was responsible for the conceptualization, validation, resources, data curation, software development, and project administration. M. Yahya, Putri Pratiwi, Hafni, Dedi Wardianto, and Asmara Yanto jointly contributed to the methodology, formal analysis, investigation, original draft preparation, review and editing, visualization, supervision, and funding acquisition. All authors have read and agreed to the published version of the manuscript.

Conflict of Interest

The author(s) declare that there are no potential conflicts of interest regarding the research, authorship, and/or publication of this article.

References

[1] BPS (Badan Pusat Statistik Indonesia), "Statistik Indonesia," Jakarta, 2023.

[2] S.K. Tilami, and S. Sampels, "Nutritional value of fish: lipids, protein, vitamin, and mineral," Reviews in Fisheries Science & Aquaculture, pp. 1-13, 2018.

[3] M. Yahya, A. Rachman, and R. Hasibuan, "Performance analysis of solar-biomass hybrid heat pump batch-type horizontal fluidized bed dryer using multi-stage heat exchanger for paddy drying," Energy, vol. 254, pp. 124294, 2022a.

[4] F. Javed, "Impact of temperature & illumination for improvement in photovoltaic system efficiency," International Journal of Smart Grid, vol. 6, no.1, pp.19-29, 2022.

[5] M. Kamruzzaman, and M.A. Abedin, "Optimization of solar cells with various shaped Surficial nanostructures," International Journal of Smart Grid, vol. 7, no.2, pp.113-118, 2023.

[6] M. Yesilbudak, and A. Ozcan, "kNN classifier applications in wind and solar energy systems," 2022 11th International Conference on Renewable Energy Research and Application (ICRERA), pp.480-484, 2022.

[7] A. Hubackova, I. Kucerova, R. Chrun, P. Chaloupkova, and J. Banout, "Development of solar drying model for selected Cambodian fish species," The Scientific World Journal, pp. 1-10, 2014.

[8] D.F. Basri, N.F. Abu Bakar, A. Fudholi, M.H. Ruslan, and Im Saroeun, "Comparison of selected metals content in cambodian striped snakehead fish (channa striata) using solar drying system and open sun drying," Journal of Environmental and Public Health, pp. 1-6, 2015.

[9] P.N. Sarsavadia, "Development of a solar assisted dryer and evaluation of energy requirement for drying of onion," Renewable Energy, vol.32, pp. 2529-2547, 2007.

[10] A.A. El-Sebaii, and S.M. Shalaby, "Experimental investigation of an indirect-mode forced convection solar

dryer for drying thymus and mint," Energy Convers Manag, vol.74, pp. 109-116, 2013.

[11] M. Yahya, "Design and performance evaluation of a solar assisted heat pump dryer integrated with biomass furnace for red chilli," International Journal of Photoenergy, pp. 1-14, 2016.

[12] M.W. Kareem, K. Habib, M.H. Ruslan, and B.B. Saha, "Thermal performance study of a multi-pass solar air heating collector system for drying of Roselle (Hibiscus sabdariffa)," Renew. Energy, vol.113, pp. 281-292, 2017.

[13] M.Yahya, R. Hasibuan, R. Sundari, and K. Sopian, "Experimental investigation of the performance of a solar dryer integrated with solid desiccant coloums using water based solar collector for medicinal herb," International Journal of Power Electronics and Drive System, vol. 12, no. 2, pp. 1024-1033, 2021.

[14] W. Wang, M. Li, R.H.E. Hassanien, and Y. Wang, "Thermal performance of indirect forced convection solar dryer and kinetics analysis of mango," Applied Thermal Engineering, vol.134, pp. 310-321, 2018.

[15] L.C. Hawa, U. Ubaidillah, A.N. Laily, N.I.W. Yosika, and F.N. Afifah, "Drying kinetics of cabya (Piper retrofractum Vahl) fruit as affected by hot water blanching under indirect forced convection solar dryer," Solar Energy, vol. 214, pp. 588-598, 2021.

[16] S. Sevik, M. Aktas, H. Dogan, and S. Kocak, "Musroom drying with solar assisted heat pump system," Energy Conversion and Management, vol. 72, pp. 171-178, 2013.

[17] K.R. Arun, G. Kunal, M. Srinivas, C.S. Sujith Kumar, M. Mohanraj, and S. Jayaraj, "Drying of untreated and in a forced musa nendra momordica charantia convection solar cabinet dryer with thermal storage," Energy, vol.192. pp. 116697, 2020.

[18] P. Moghimi, H. Rahimzadeh, and A. Ahmadpour, "Experimental and numerical optimal design of a household solar fruit and vegetable dryer," Solar Energy, vol. 214, pp. 575-587, 2021.

[19] M. Mohanraj, "Performance of a solar-ambient hybrid source heat pump drier for copra drying under hot-humid weather conditions," Energy for Sustainable Development, vol. 23, pp. 165-169, 2014.

[20] J. Prasad, and V.K. Vijay, "Experimental studies on drying of Zingiber officinale, Curcuma l. and Tinosopora cardifolia in solar-biomass hybrid dryer," Renewable Energy, vol. 30, pp. 2097-2109, 2005.

[21] M. Mohanraj, and P. Chandrasekar, "Comparison of drying characteristics and quality of copra obtained in a forced convection solar drier and sun drying," Journal of Scientific and Industrial Research, vol. 67, no. 5, pp. 381-385, 2008.

[22] G. Mallikarjuna, V.V.R. Mugi, V.P. Chandramohan, and S. Suresh, "A novel indirect solar dryer with inlet fans powered by solar PV panels: Drying kinetics of Capsicum Annum and Abelmoschus esculentus with dryer performance," Solar Energy, vol. 194, pp. 871-885, 2019.

[23] A. Lingayat, V.P. Chandramohan, and V.R.K. Raju, "Energy and exergy Analysis on drying of banana using indirect type natural convection solar dryer," Heat Transfer Engineering, vol. 41, no. (6-7), pp. 551-561, 2019.

[24] B.K. Bala, and M.R.A. Mondol, "Experimental investigation on solar drying of fish using solar tunnel dryer," Drying Technology, vol. 19, no.2, pp. 427-436, 2001.

[25] A. Fudholi, B. Bakhtyar, H. Saleh, M.H. Ruslan, M.Y. Othman, and K. Sopian. Drying of salted silver jewfish in a hybrid solar drying system and under open sun: Modeling and performance analyses. International Journal of Green Energy, vol. 13, no. 11, pp. 1135-1144, 2016.

[26] Hamdani, T.A. Rizal, and M. Zulfri, "Fabrication and testing of hybrid solar-biomass dryer for drying fish," Case Studies in Thermal Engineering, vol. 12, pp. 498-496, 2018.

[27] R. Echazu, L. Saravia, and M. Condori, "Solar drying of sweet pepper and garlic using the tunnel greenhouse drier," Renewable Energy, vol. 22, pp. 447-460, 2001.

[28] A. Kumar, and G.N. Tiwari, "Effect of mass on convective mass transfer coefficient during open sun and greenhouse drying of onion flakes," Journal of Food Engineering, vol. 79, pp. 1337-1350, 2007.

[29] S. Nayak, A. Kumar, J. Mishra, and G.N. Tiwari, "Drying and testing of mint (Mentha piperita) by a hybrid photovoltaic-thermal (PVT)-based greenhouse dryer," Drying Technology, vol. 29, no. 9, pp. 1002-1009, 2011.

[30] M.M. Morad, M.A. El-Shazly, K.I. Wasfy, and H.A.M. El-Maghawry, "Thermal analysis and performance evaluation of a solar tunnel greenhouse dryer for drying peppermint plants," Renewable Energy, vol. 101, pp. 991-1004, 2017.

[31] J. Kaewkiew, S. Nabnean, and S. Janjai, "Experimental investigation of the performance of a large-scale greenhouse type solar dryer for drying chilli in Thailand," Procedia Engineering, vol. 32, pp. 433-439, 2012.

[32] E. Aritesty, and D. Wulandani, "Performance of the rack type-greenhouse effect solar dryer for wild ginger (curcuma xanthorizza roxb.) drying," Energy Procedia, vol. 47, pp. 94-100, 2014.

[33] T.C. Tham, Ng.M. Xiang, S.H. Gan, L.S. Chua, R. Aziz, and L.A. Chuah, "Effect of ambient conditions on drying of herbs in solar greenhouse dryer with integrated heat pump," Drying Technology, vol. 35, no. 14, pp. 1721-1732, 2017.

[34] Z. Azaizia, S. Kooli, A. Elkhadraoui, I. Hamdi, and A.A. Guizani, "Investigation of a new solar greenhouse drying system for peppers," International Journal of Hydrogen Energy, vol. 42, no. 13, pp. 8818-8826, 2017.

[35] P. Hempattarasuwan, P. Somsong, K. Duangmal, M. Jaskulski, J. Adamiec, and G. Srzednicki, "Performance evaluation of parabolic greenhouse-type solar dryer used for drying of cayenne pepper," Drying Technology, pp. 48-54, 2019.

[36] P. Barnwal, and G.N. Tiwari, "Grape drying by using hybrid photovoltaic-thermal (PV/T) greenhouse dryer: An experimental study," Solar Energy, vol. 82, no. 12, pp. 1131-1144, 2008.

[37] N.S. Rathore, and N.L. Panwar, "Experimental studies on hemi cylindrical walk-in type solar tunnel dryer for grape drying," Applied Energy, vol. 87, no. 8, pp. 2764-2767, 2010.

[38] P.S. Chauhan, and A. Kumar, "Thermal modeling and drying kinetics of gooseberry drying inside north wall insulated greenhouse dryer," Applied Thermal Engineering, vol.130, pp. 587-597, 2018a.

[39] D. Jain, and G. Tiwari, "Effect of greenhouse on crop drying under natural and forced convection I: Evaluation of convective mass transfer coefficient," Energy Conversion and Management, vol.45, pp. 765-783, 2004.

[40] G.N. Tiwari, S. Kumar, and O. Prakash, "Evaluation of convective mass transfer coefficient during drying of jaggery," Journal of Food Engineering, vol.63, no. 2, pp. 219-227, 2004.

[41] T. Ratnawati, "Simulasi model pengering efek rumah kaca untuk pengeringan cengkeh (Eugenia caryophyllus)," Jurusan Teknik Pertanian, Fakultas Teknologi Pertanian, Institut Pertanian Bogor, 2023.

[42] P. Vijaykumar, S.R. Desai, Lokesh, and M. Anantachar, "Performance evaluation of solar tunnel dryer for chilly drying. Karnataka J. Agric. Sci, vol.25, no. 4, pp. 472-474, 2012.

[43] S. Soponronnarit, and S. Prachayawarakorn, "Optimum strategy for fluidized bed paddy drying," Drying Technology, vol.12, no. 7, pp. 1667-1686, 1994.

[44] H. Darvishi, M. Azadbakht, and B. Noralahi, "Experimental performance of mushroom fluidized-bed drying: Effect of osmotic pretreatment and air recirculation," Renewable Energy, vol. 120, pp. 201-208, 2018.

[45] M. Yahya, H. Fahmi, A. Fudholi, and K. Sopian, "Performance and economic analyses on solar-assisted heat pump fluidised bed dryer integrated with biomass furnace for rice drying," Solar Energy, vol. 174, pp. 1058–1067, 2018.

[46] S.Z. Ilyas, A. Hassan, and H. Mufti, "Review of the renewable energy status and prospects in Pakistan," International Journal of Smart Grid, vol. 5, no.4, pp.167-173, 2021.

[47] F.M. Wulfran, D.N.S. Raoul, M.R.J. Jacques, and K.T. Saatong, "A technical analysis of a grid-connected hybrid renewable energy system under meteorological constraints for a timely energy management," International Journal of Smart Grid, vol. 7, no.2, pp.53-60, 2023.

[48] R.J.J. Molu, S.R.D. Naoussı, P. Wıra, W.F. Mbasso, and S.K. Tsobze, "Solar irradiance forecasting based on deep learning for sustainable electrical energy in Cameroon," International Journal of Smart Grid, vol. 7, no.2, pp.61-68, 2023.

[49] E.K. Akpinar, "Drying of mint leaves in solar dryer and under open sun: Modelling, performance analyses," Energy Conversion and Management, vol. 51, pp. 2407-2418, 2010.

[50] M. Yahya, H. Fahmi, R. Hasibuan, and A. Fudholi, "Development of hybrid solar-assisted heat pump dryer for drying paddy," Case Studies in Thermal Engineering, vol. 45, pp. 102936, 2023.

[51] A. Fudholi, M.Y. Othman, M.H. Ruslan, and K. Sopian, "Drying of Malaysian Capsicum annuum L. (red chili) dried by open and solar drying," Int. J. Photoenergy, pp. 1-9, 2013.

[52] A. Fudholi, K. Sopian, M.Y. Othman, and M.H. Ruslan, "Energy and exergy analyses of solar drying system of red seaweed," Energy and Building, vol. 68, pp. 121-129, 2014a.

[53] S. Mehran, M. Nikian, M. Ghazi, H. Zareiforoush, and I. Bagheri, "Experimental investigation and energy analysis of a solar-assisted fluidizedbed dryer including solar water heater and solar-powered infrared lamp for paddy grains drying," Solar Energy, vol. 190, pp. 167-184, 2019.

[54] M. Yahya, H. Fahmi, and H. Hasibuan, "Experimental performance analysis of a pilot-scale biomass-assisted recirculating mixed-flow dryer for drying paddy," International Journal of Food Science, pp. 1-15, 2022b.

[55] A. Fudholi, K. Sopian, M.A. Alghoul, M.H. Ruslan, and M.Y. Othman, "Performances and improvement potential of solar drying system for palm oil fronds," Renewable Energy, vol. 78, pp. 561-565, 2015.

[56] M.M.A. Khan, A. Sayem, and M.M. Asan, "Experimental investigations of a simple and cheap passive solar dryer for preserving agricultural products," International Journal of Renewable Energy Research, vol. 12, no.4, pp. 2102-2110, 2022.